Influence of excitation conditions in an alternating field on kinetic and dielectric characteristics intercalated compounds Ag$_x$MoSe$_2$

© V.G. Pleshchev

Institute of Natural Sciences and Mathematics, Ural Federal University,
Yekaterinburg, Russia

E-mail: v.g.pleshchev@urfu.ru

Using the technique of impedance spectroscopy, data on the effect of the magnitude of the variable signal and the constant bias on the kinetic characteristics of the Ag$_x$MoSe$_2$ samples were obtained. The effect of temperature on the parameters of the impedance spectra of the studied compounds and on their dielectric characteristics, which were analyzed within the framework of the electrical modulus formalism, is also shown.

Keywords: impedance, intercalates, molybdenum diselenide, silver, permittivity, electric modulus.

1. Introduction

Transition metal dichalcogenides with general formula MX_2 feature a lamellar structure where structural fragments (sandwiches) MX_2 are weakly bonded via weak Van der Waals interaction [1–3]. Structural features of such materials enable their properties to be modified by intercalation of atoms between layers MX_2 of atoms in other element atoms.

Kinetic and magnetic properties of such materials have been investigated earlier using dichalcogenides of group 4 and 5 of the periodic table intercalated with 3d-transition metals [4–7] and group 1 atoms (copper and silver) [8–11]. Important difference of the second group intercalants is in that ions of group 1 elements having a closed electron shell do not tend to establish covalent bonds with molecular orbitals MX_2 and, as a result, are weakly bound in the interlayer space [12].

Molybdenum dichalcogenides also have these structural features and being low-dimensional structure materials are used as the basis for microelectronics devices [13,14]. Unlike titanium diselenide, molybdenum diselenide may have various structural modifications (polytypes) such as 2H-MoSe$_2$ and 3R-MoSe$_2$ which differ in atom positions and number of MoSe$_2$ layers in the lattice cell. 2H-MoSe$_2$ modification is described within a hexagonal structure (SG: $P6_3/mmc$). 2H-MoSe$_2$ lattice cell contains two MoSe$_2$ layers with trigonal prismatic environment of molybdenum atoms.

Another difference is in that materials based on titanium dichalcogenides usually had metallic type conduction, and for materials based on hafnium or molybdenum dichalcogenides, conduction dependence is of activation type [8,10]. The existing experimental data obtained using AC and DC current showed that hopping conduction mechanism can be implemented in such compounds and described in accordance with the Mott model with variable hop length [9,15]. The activation type conduction shall depend on charge carrier excitation conditions, including excitation from AC signal amplitude, DC field presence and strength, experiment temperature conditions and other environmental factors. Detected polarization phenomena in Ag-HfSe$_2$ [16] compounds provide the basis for investigation of dielectric behavior of intercalated silver-containing materials like in a set of earlier studies [17–19].

This study is devoted to the investigation of kinetic and dielectric properties of molybdenum diselenide intercalated with silver atoms.

2. Experiment

Polycrystalline Ag$_x$MoSe$_2$ $(x = 0.1; 0.2)$ samples were synthesized by solid-state reaction method in evacuated quartz vessels made from preliminary prepared molybdenum diselenide and required calculated amount of metallic silver. Such process has been used multiple times before for synthesis of intercalated materials [5–8]. From our experience, this allowed to avoid direct interaction between free selenium and silver which is enabled when the samples are synthesized from initial elements. After a set of homogenizing annealing, X-ray qualification of the initial MoSe$_2$ matrix and intercalated samples was carried out using Bruker D8 Advance diffractometer in CuK_α-radiation, and formation of 2H-structural modification in them was proved.

AC measurements were carried out at various temperatures $(296-333\,\text{K})$ using Solartron 1260A multi-purpose frequency response analyzer in linear frequency range (f) $10\,\text{Hz}-5\,\text{MHz}$. AC signal U_{ac} varied from 0.1 to 0.5 V. Difference of DC potential U_{dc} varied from zero to 0.5 V. Real and imaginary parts of permittivity were determined from impedance data and geometrical capacity of the utilized cell [20]. The analysis was carried out within an

equivalent scheme with resistor and capacitor connected in parallel.

3. Results

Figure 1, a and 2, a shows low-frequency fragments of complex impedance spectra for $Ag_{0.1}MoSe_2$ and $Ag_{0.2}MoSe_2$ samples obtained at various AC signals $U_{ac} = 0.1\,V$ and $U_{ac} = 0.5\,V$ (curves $1, 2$) and additionally applied DC voltage $U_{dc} = 0.5\,V$ (curve 3). It can be seen that with increase in U_{ac}, right portions of the spectra move to the left and exhibit reduced active resistance R_a. Additional spectrum shift also occurs when additional DC voltage is applied. The behavior of real Z' and imaginary Z'' impedance components depending on frequency with varied
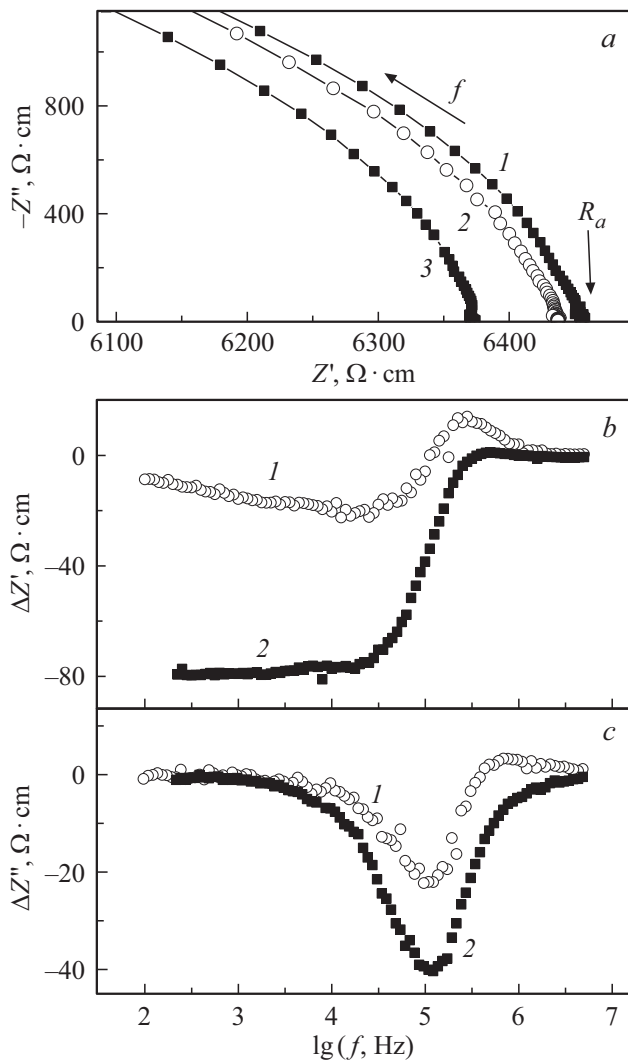
Figure 1. a — low frequency spectrum portions of $Ag_{0.1}MoSe_2$ complex impedance at different excitation levels: $U_{ac} = 0.1\,V$ (1), $U_{ac} = 0.5\,V$ (2), $U_{ac} = 0.5\,V + U_{dc} = 0.5\,V$ (3); b, c — frequency dependences of the difference of real (b) and imaginary (c) complex impedance components between curves 2 and 1 (1) and curves 3 and 2 (2) as shown in Figure 1, a.
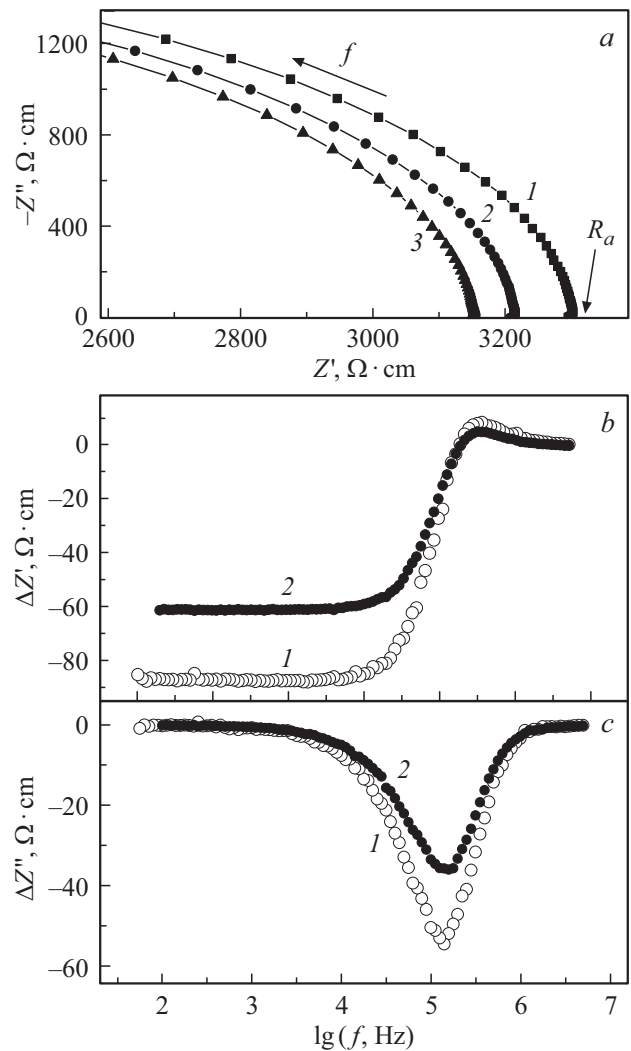
Figure 2. a — low frequency spectrum portions of $Ag_{0.2}MoSe_2$ complex impedance at different excitation levels: $U_{ac} = 0.1\,V$ (1), $U_{ac} = 0.5\,V$ (2), $U_{ac} = 0.5\,V + U_{dc} = 0.5\,V$ (3); b, c — frequency dependences of the difference of real (b) and imaginary (c) complex impedance components between curves 2 and 1 (1) and curves 3 and 2 (2) as shown in Figure 2, a.

excitation level is also shown in more detail in Figure 1, b and 1, c for $Ag_{0.1}MoSe_2$ and in Figure 2, b and 2, c for $Ag_{0.2}MoSe_2$ in the form of differences $\Delta Z'$ and $\Delta Z''$. Curves $\Delta Z'(f)$ show the behavior of spectra positions on the complex plane on the x axis. According to the data, all difference within the high frequency limit are reduced to zero.

Dependences $\Delta Z''(f)$ shown in Figure 1, c and Figure 2, c exhibit a minimum indicating the decrease in spectra maximum Z''_{max} with the increase in the excitation level. At the same time, Z''_{max} position on the frequency scale for each of the samples is almost unchanged, which is indicative of permanent relaxation times during charge transfer at various excitation signal characteristics. However, it can be seen that with the increase in silver content, minimum $\Delta Z''$ value moves to a higher frequency region
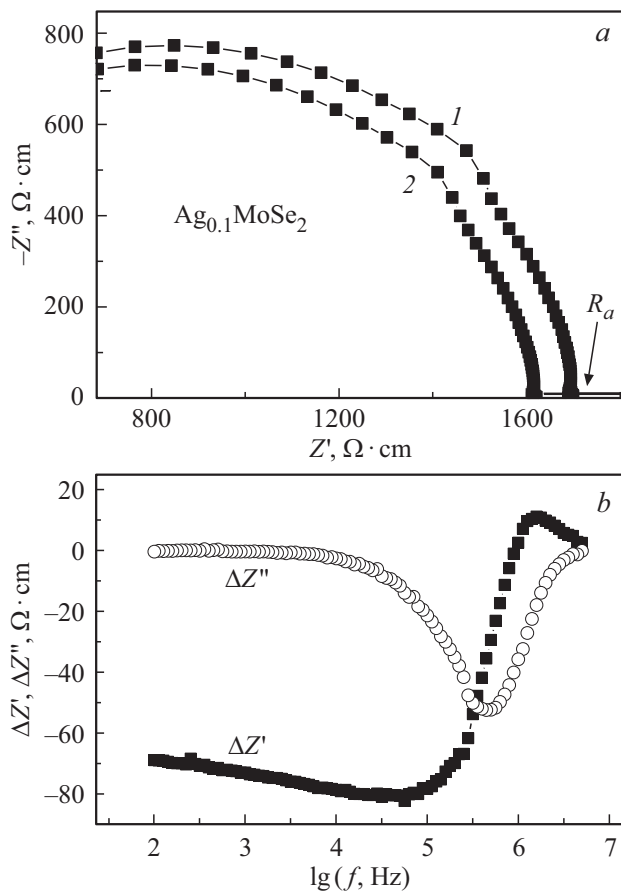
Figure 3. a — $Ag_{0.1}MoSe_2$ impedance spectra at $T = 333$ K and $U_{ac} = 0.1$ V (1) and $U_{ac} = 0.5$ V (2); b — frequency dependences of variation of real and imaginary impedance components.

reflecting the acceleration of relaxation processes. The conducted investigations suggest that variation of charge carrier excitation level in these compounds does not change the charge transfer mechanism itself, but only increases the probability of overcoming potential barriers when charge carriers are activated.

The provided data shows that conduction increase with silver content growth in samples occurs due to charge carrier concentration growth, on the one hand, and increase in carrier mobility, on the other hand, which is indicated by the reduced relaxation time. Thanks to the activation nature of conduction, kinetic properties of the studied compounds may be also influenced, besides excitation variation, by temperature variation. This influence is illustrated in Figure 3 showing the results obtained for $Ag_{0.1}MoSe_2$ at $T = 333$ K and at $U_{ac} = 0.1$ V and $U_{ac} = 0.5$ V. Figure 3, a shows complex impedance spectra which clearly demonstrate their difference at different excitation levels. Temperature rise causes reduction of active resistance of the sample and movement of maximum Z'' to the higher frequency region, which defines reduction of relaxation time. When comparing data for $Ag_{0.1}MoSe_2$ obtained at two temperatures, it may be noted that, taking into account

considerable reduction of Z' and Z'' with temperature rise, increase in the AC amplitude results in relatively high variation of these values compared with similar variations at $T = 296$ K. In this case, increase in probability of thermal fluctuations also facilitates the increase in charge carrier mobility.

To investigate dielectric response of the studied compounds on the basis of the impedance data, real (ε') and imaginary (ε'') components of the complex dielectric constant were calculated [20].

The calculations has shown that significant frequency dispersion of the complex dielectric constant components is present. Figures 4 and 5 show that ε'' values characterizing the energy loss in AC field decrease steadily for both samples with frequency growth. Such behavior of dependences was also detected in hafnium diselenide intercalated with copper atoms [17] and in silver-containing
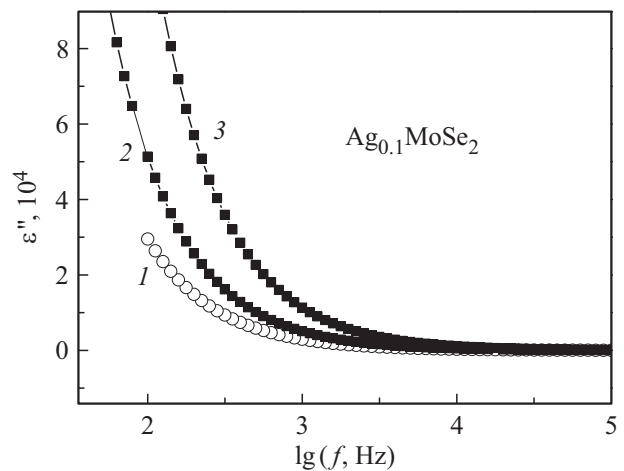
Figure 4. Frequency dependences of imaginary permittivity components $Ag_{0.1}MoSe_2$ at different temperatures: 296 (1), 313 (2), 333 K (3).
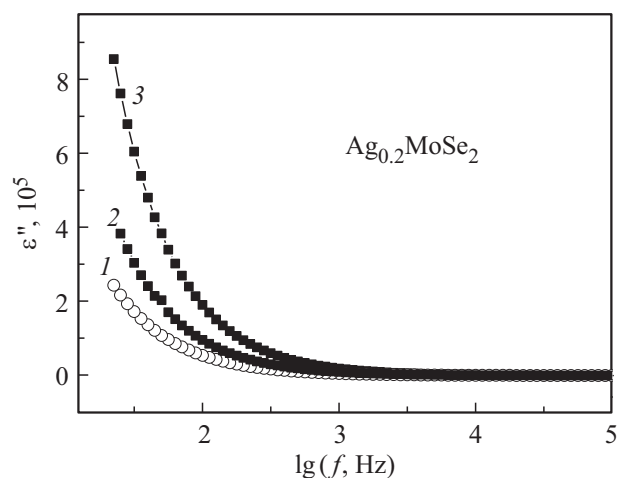
Figure 5. Frequency dependences of imaginary permittivity components $Ag_{0.2}MoSe_2$ at different temperatures: 296 (1), 313 (2), 333 K (3).
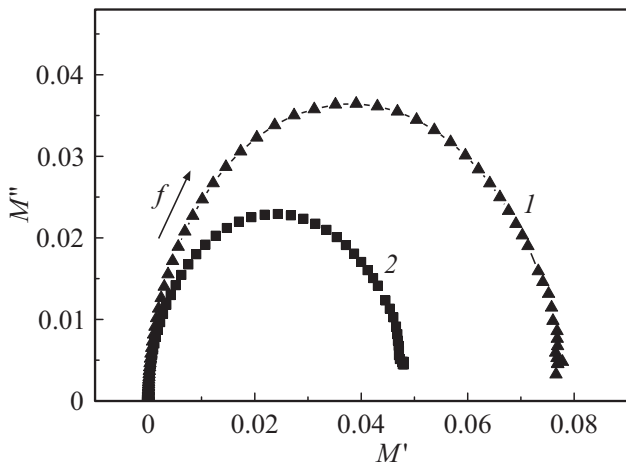
Figure 6. Complex electrical modulus spectra $Ag_{0.1}MoSe_2$ (*1*) and $Ag_{0.2}MoSe_2$ (*2*) at $T = 296$ K.

hafnium disulphide [18]. High ε'' at low frequencies may be caused by polarization effects which may be specific to ion-conducting materials [16,21]. The observed behavior of the dependences shows that there is dielectric relaxation in $Ag_x MoSe_2$. However, no dielectric loss maxima associated with this relaxation have been detected in the measurement frequency range. The absence of maximum on frequency dependences ε'' indicates that conduction loss prevails among the energy loss mechanism in the studied samples. In this case, the inherent dielectric behavior of the studied materials may be hidden and the obtained data may not be used to assess the dielectric relaxation characteristics. Such problem, according to literature, can be solved when the results are represented in the form of electrical modulus [22–24] whose complex value is inverse to complex permittivity $M^* = 1/\varepsilon^* = M' + iM''$. Each of the components is calculated as $M' = \varepsilon'/(\varepsilon'^2 + \varepsilon''^2)$ and
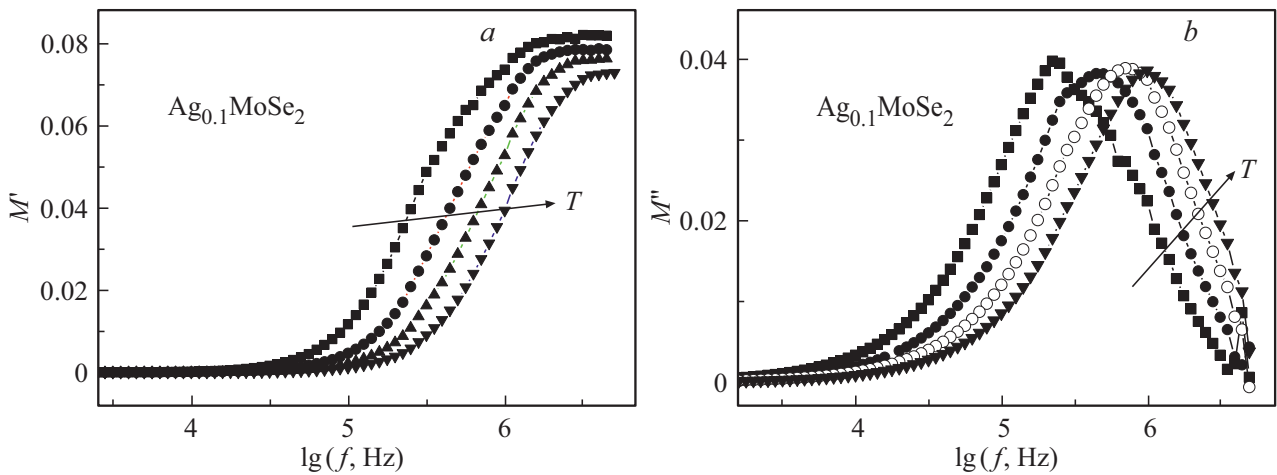
Figure 7. Frequency dependences of real (*a*) and imaginary (*b*) components of the electrical modulus of $Ag_{0.1}MoSe_2$ at different temperatures: 296, 313, 323 and 333 K).
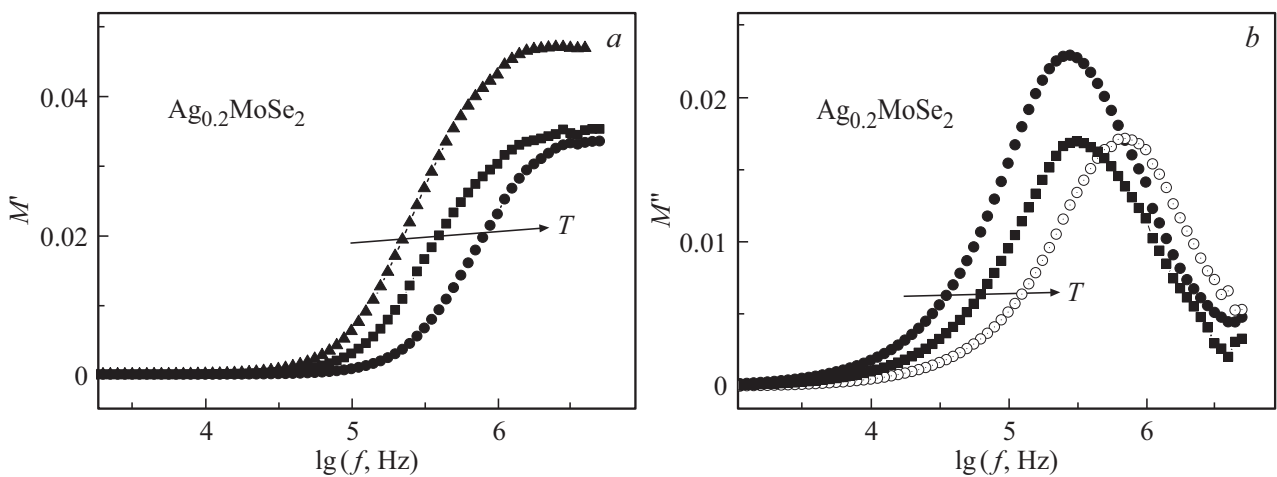
Figure 8. Frequency dependences of real (*a*) and imaginary (*b*) components of the electrical modulus of $Ag_{0.2}MoSe_2$ at different temperatures: 296, 313 and 333 K.

High frequency permittivity (ε_∞) and dielectric relaxation times (τ_ε) $Ag_{0.1}MoSe_2$ and $Ag_{0.2}MoSe_2$ at various temperatures

T	$Ag_{0.1}MoSe_2$		$Ag_{0.2}MoSe_2$	
	ε_∞	τ_ε, μs	ε_∞	τ_ε, μs
296	12.3	0.64	21.3	0.58
313	12.8	0.36	28.6	0.48
323	13.15	0.23	28.9	0.46
333	13.75	0.16	30.3	0.23

$M'' = \varepsilon''/(\varepsilon'^2 + \varepsilon''^2)$ [20]. In this case the imaginary part of electrical modulus transforms the low-frequency growth of permittivity into a relaxation peak whose position allows to determine the dielectric relaxation time.

Actually, such transformations gave the complex-plane electrical modulus spectra in the form of the arc of a circle (Figure 6). Frequency dependences of the real and imaginary components of the electrical modulus as shown in Figures 7 and 8 at different temperatures provide more detailed information. Figures 7, *a* and 8, *a* show that M' at $f \rightarrow \infty$ asymptotically approach to their maximum values. This allows to derive high frequency permittivity at different temperatures as $\varepsilon_\infty = 1/M'_{max}$ (see the Table).

Figure 7, *b* and 8, *b* show dependences M'' on frequency having their maxima at certain frequencies f_{max}. It can be seen that temperature rise causes movement of position M''_{max} to the higher frequency region which indicates that the dielectric relaxation time is reduced as may be defined as $\tau_\varepsilon = (2\pi f_{max})^{-1}$. The obtained data is also given in the Table.

4. Conclusion

The study demonstrates the influence of AC field amplitude on the shape and characteristics of $Ag_{0.1}MoSe_2$ and $Ag_{0.2}MoSe_2$ impedance spectra. It is shown that increasing AC filed amplitudes causes the impedance spectrum shift on the complex plane. At the same time, active resistance R_a decreased. Additionally applied DC field caused further reduction of R_a. Detailed analysis of frequency dependences of those changes in the real and imaginary components of the complex impedance that accompany the excitation level variation. It has been noted that maximum of the imaginary impedance component for both samples decreases with increase in the excitation level, though, the position of this maximum on the frequency scale remains almost unchanged. These data shows that the relaxation times during charge transfer are unchanged, and the active resistance reduction is caused by the increased probability of activation processes during charge transfer with increasing AC and DC fields. Temperature rise causes further reduction of active resistance and relatively more significant changes in the complex impedance components.

The use of impedance data for the investigation of dielectric characteristics of Ag_xMoSe_2 is the new result of the study. Since the imaginary component of the complex permittivity did not exhibit a typical maximum on its frequency curve, a prevailing energy loss mechanism associated with charge transfer (conduction) in the AC field was suggested. Therefore, the analysis of dielectric characteristics was carried out in term of the electrical modulus which allowed to represent the dielectric response as a characteristic spectrum on the complex plane. Frequency dependences of real and imaginary components of the electrical module allowed to determine the dielectric relaxation times and assess high frequency permittivity of $Ag_{0.1}MoSe_2$ and $Ag_{0.2}MoSe_2$ at different temperatures.

Conflict of interest

The author declares that he has no conflict of interest.

References

[1] A. Wilson, A.D. Yoffe. Adv. Phys. **18**, 193 (1969).
[2] W. Choi, N. Choudhary, J. Park, G.H. Han, Y.H. Lii, D. Akinwande. Mater. Today **20**, *3*, 116 (2017). DOI: 10.1016/j.mattod.2016.10.002
[3] L.A. Chernozatonsky, A.A. Artyukh. UFN **188**, *1*, 3 (2018). (in Russian). DOI: 10.3367/UFNr.2017.02.038065
[4] V.I. Maksimov, N.V. Baranov, V.G. Pleshchev, K. Inoue. J. Alloys Comp. **384**, 33 (2004). DOI: 10.1016/j.jallcom.2004.03.129
[5] V.G. Pleshcheev, N.V. Baranov, I.A. Martyanova. FTT **48**, *10*, 1843 (2006). (in Russian).
[6] E.M. Sherokalova, N.V. Selezneva, V.G. Pleshchev. FTT **64**, *4*, 437 (2022). (in Russian). DOI: 10.21883/FTT.2022.04.52183.256
[7] V.G. Pleshchev, N.V. Selezneva. FTT **60**, *2*, 245 (2018). (in Russian). DOI: 10.21883/FTT.2018.02.45375.219
[8] V.G. Pleshchev, N.V. Selezneva, N.V. Baranov. FTT **55**, *7*, 1281 (2013). (in Russian).
[9] V.G. Pleshchev, N.V. Selezneva, N.V. Melnikova, N.V. Baranov. FTT **54**, *7*, 1271 (2012). (in Russian).
[10] V.G. Pleshchev, N.V. Melnikova, N.V. Baranov. FTT **57**, *8*, 1473 (2015). (in Russian).
[11] V.G. Pleshchev, N.V. Melnikova. FTT **56**, *9*, 1702 (2014). (in Russian).
[12] A.H. Rechak, S. Auluk. Physica B **363**, 25 (2005). DOI: 10.1016/j.physb.2005.02.030
[13] C.K. Sumesh, K.D. Patel, V.M. Pathak, R. Srivastava. J. Electron Dev. **8**, 324 (2010).
[14] Y.C. Lee, D.L. Shen, K.W. Chen, W.Z. Lee, S.Y. Hu, K.K. Tiong, Y.S. Huang. J. Appl. Phys. **99**, *6*, 63706(5) (2006). https://doi.org/10.1063/1.2180398
[15] N. Mott, E. Davis. Eletronnye protsessy v nekristallicheskikh veshchestvakh. Mir, M. (1982). V. 1. 368 p. (in Russian).
[16] V.G. Pleshchev, N.V. Selezneva, N.V. Baranov. FTT **55**, *1*, 14 (2013). (in Russian).

[17] V.G. Pleshchev. IOSR J. Appl. Phys. **13**, *5*, 33 (2021). DOI: 10.9790/4861-1305013336

[18] V.G. Pleshchev. FTT **65**, *2*, 232 (2023). (in Russian). DOI: 1021883/FTT.2023.02.54295.520

[19] S.M. Asadov, S.N. Mustafaeva. Neorgan. materialy **55**, *11*, 1151 (2019) DOI: 10.1134/S0002337X19100014

[20] N.A. Poklonsky, N.I. Gorbachuk. Osnovy impedansnoy spektroskopii kompozitov. Publishing House of Belarusian State University, Minsk (2005). 150 p. (in Russian).

[21] .B. Louati, K. Guidara, M. Gargouri. J. Alloys Comp., **472**, 347 (2009). DOI: 10.1016/j.jallcom.2008.04.050

[22] A.M. Solodukha, Z.A. Liberman. Vestn. Boronezhskogo gos. un-ta. Ser. Fizika, Matematika **2**, 67 (2003). (in Russian).

[23] M.Yu. Seyidov, R.A. Suleymanov, Y. Bakis, F. Salehli. J. Appl. Phys. **108**, *7*, 074114(5) (2010). DOI: 10.1063/1.3486219

[24] M.A. Kudryashov, A.I. Mashin, A.A. Logunov, G. Chidichimo, G. De Filpo. ZhTF **84**, *7*, 67 (2014). (in Russian).

Translated by E.Ilyinskaya